New Journal of Chemistry

Zinc(II) and Cadmium(II) Complexes, [M(^{i}Pr$_2$P(X)NC(Y)NC$_5$H$_{10}$-κ^2-*X,Y*)$_2$] (X and Y= O, S), as Single Source Precursors for Metal Sulfide Thin films

Víctor Flores-Romero, Oscar L. García-Guzmán, Alejandra Aguirre-Bautista, Iván D. Rojas-Montoya, Verónica García-Montalvo,* Margarita Rivera, Omar Jiménez-Sandoval, Miguel-Ángel Muñoz-Hernández and Simón Hernández-Ortega.

Content:

1. Table S1. Crystallographic Data for compounds **2**, **6**, **7** and **9**

Compound	**2**	**6**	**7**	**9**
Formula	$C_{12}H_{25}N_2OPS$	$C_{24}H_{48}N_4O_2P_2S_2Zn$	$C_{24}H_{48}CdN_4P_2S_4$	$C_{24}H_{48}CdN_4O_2P_2S_2$
M [g/mol]	276.37	616.09	695.24	663.12
Crystal size (mm)	0.463 x 0.312 x 0.246	0.407 x 0.307 x 0.174	0.516 x 0.316 x 0.144	0.299 x 0.250 x 0.112
Crystal system	Monoclinic	Monoclinic	Triclinic	Monoclinic
Space group	C 2/c (15)	$P2_1/n$ (14)	P-1 (2)	$P2_1/n$ (14)
ρ_{calc} (g cm^{-3})	1.129	1.296	1.390	1.372
Z	8	4	2	4
***a* (Å)**	10.0025(6)	11.9623(2)	9.9720(2)	11.9249(2)
***b* (Å)**	18.7416(11)	11.1902(2)	13.3201(2)	11.0983(2)
***c* (Å)**	17.4507(10)	23.5940(3)	13.5216(2)	24.2600(5)
α (°)	90.00	90.00	86.0570(10)	90.00
β (°)	96.041(2)	91.5400(10)	68.82 (10)	90.3960(10)
γ (°)	90.00	90.00	82.7220(10)	90.00
***V* (Å^3)**	3253.2(3)	3157.16(9)	1660.72(5)	3210.64(10)
μ (mm^{-1})	0.287	1.038	1.025	0.936
***F*(000)**	1200	1312	724	1384
Reflections Collected	19321	27833	19444	15124
Unique reflections R_{int}	2981; 0.0395	5765, 0.0399	6095, 0.0281	5884; 0.0365
***R*1, *wR*2 [I>2σ(I)]**	0.0467; 0.1274	0.0296; 0.0751	0.0288, 0.0757	0.0299; 0.0597
***R*1, *wR*2 (all data)**	0.0559; 0.1346	0.0389; 0.0787	0.0352, 0.0799	0.0482; 0.0670
Correction Method	None	Analytical	Analytical	Analytical
GooF	1.054	1.036	1.052	0.949

2. Figure S1. Micrographs of as-deposited and annealed ZnS thin films: 4F, 5F and 6F (unannealed) and 4Fa, 5Fa and 6Fa (annealed).

AFM micrograph(10 x 10 µm): **4F**

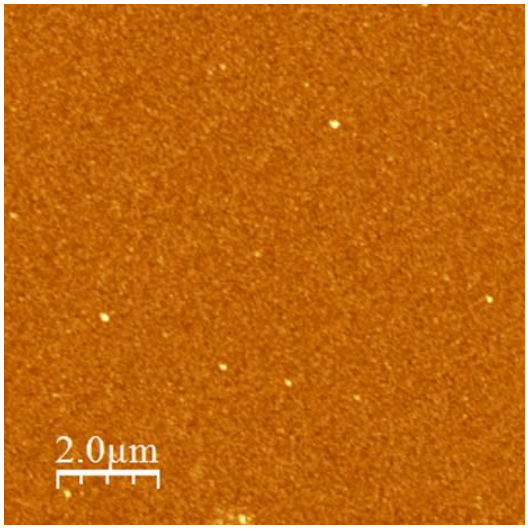

AFM micrograph (10 x 10 µm)**:4Fa**

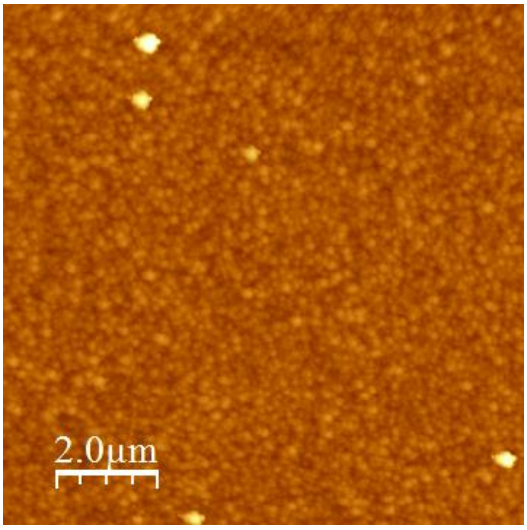

Low (inset) and high magn. SEM images: **4Fa** and : **5F**

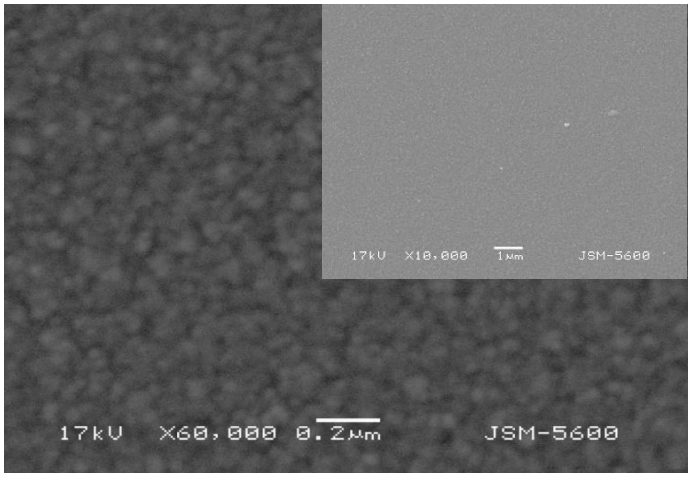

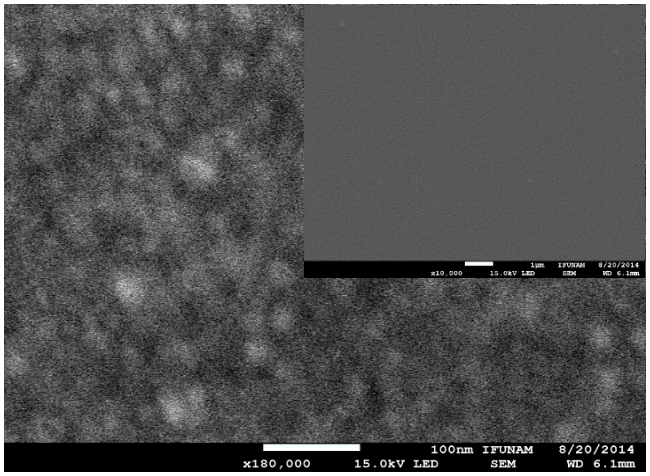

5F: Elemental Mapping (SEM), sulfur and zinc distribution.

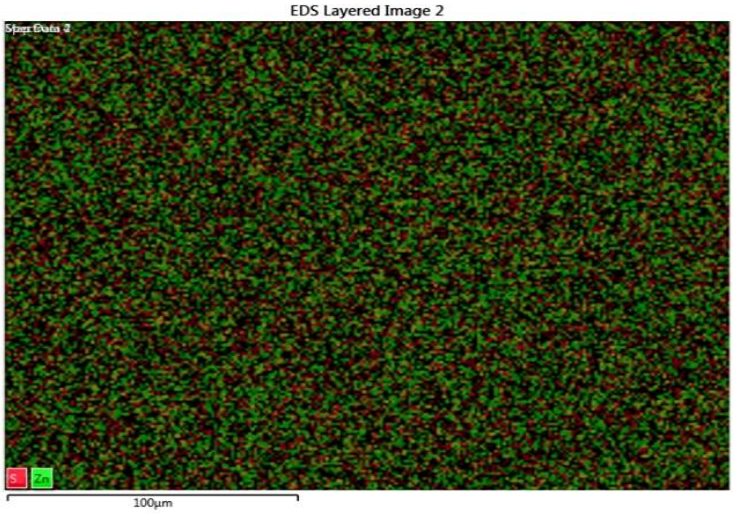

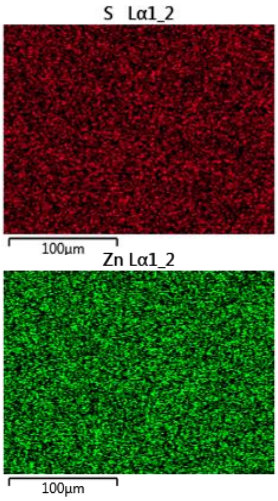

Low (inset) and high magn. SEM images: **5Fa**

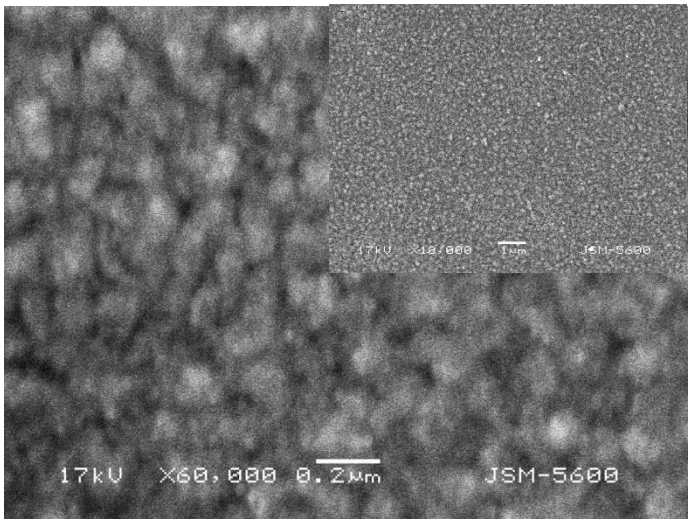

AFM (1 x 1 μm, inset10 x 10 μm): **5Fa**

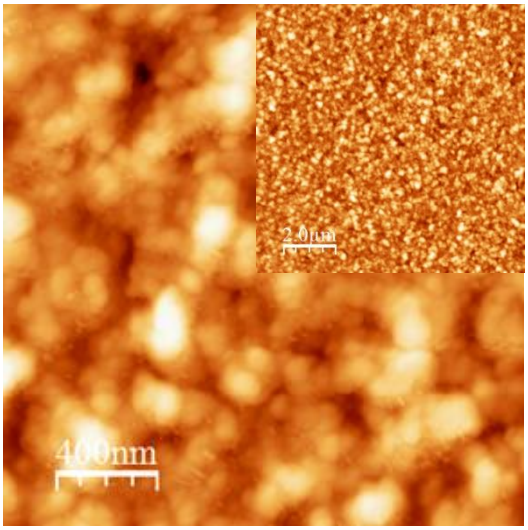

Low (inset) and high magnification SEM images: **6F**

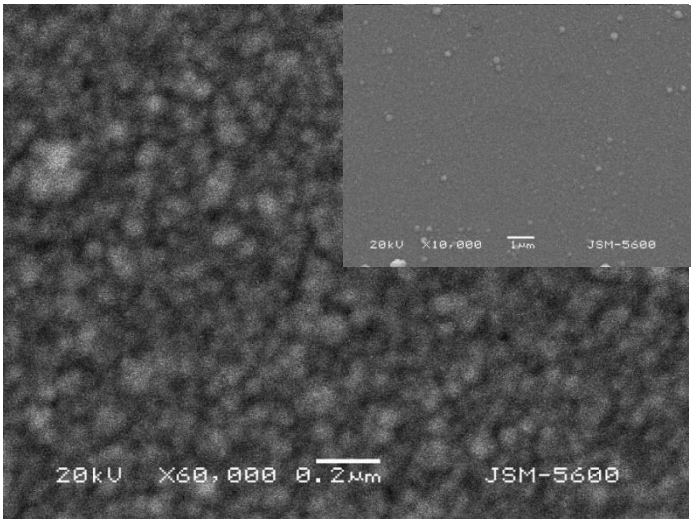

AFM micrograph (10 x 10 μm): **6F**

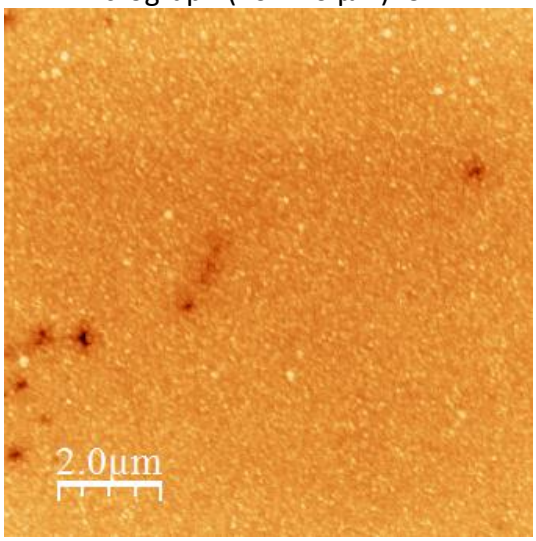

Low (inset) and high magnification SEM images: **6Fa**

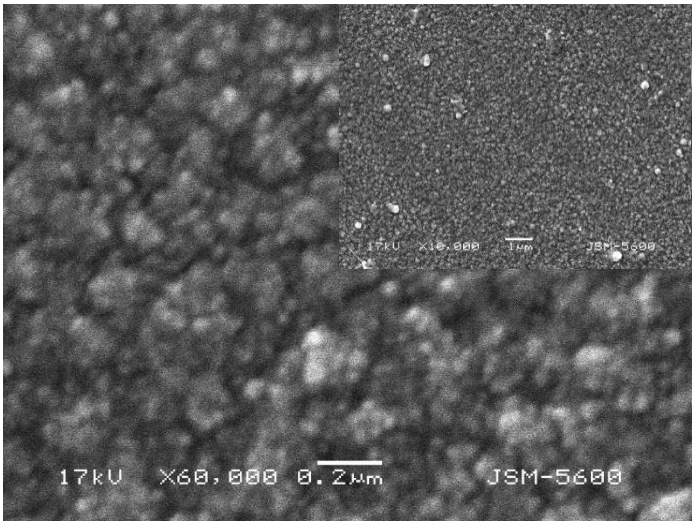

AFM micrograph (1 x 1 μm, inset10 x 10 μm): **6Fa**

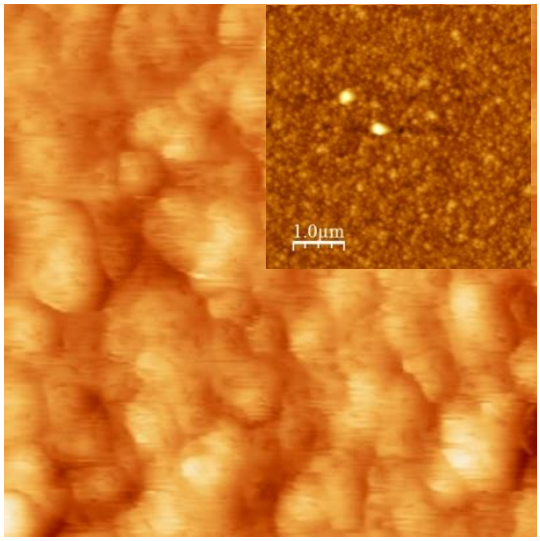

3. Figure S2. Micrographs of as-deposited and annealed CdS thin films: 7F, 8F and 9F (unannealed) and 7Fa, 8Fa and 9Fa (annealed) and AFM micrograps of annealed 8Fa and 9Fa.

FM micrograph(10 x 10 µm): **7F**

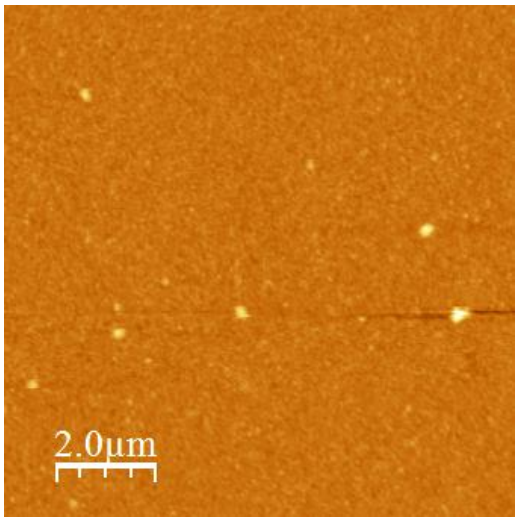

AFM micrograph (10 x 10 µm)**:7Fa**

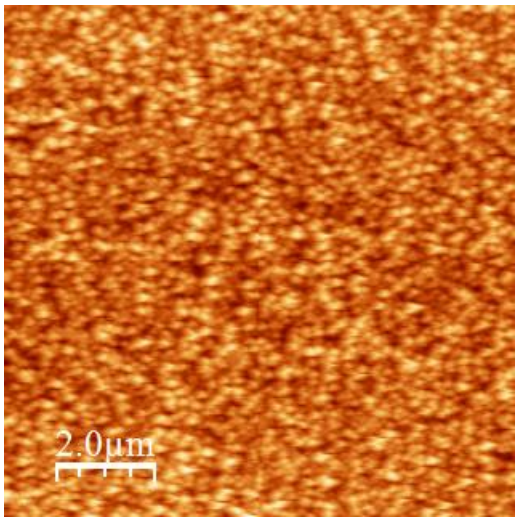

7F: Elemental Mapping (SEM), sulfur and zinc distribution

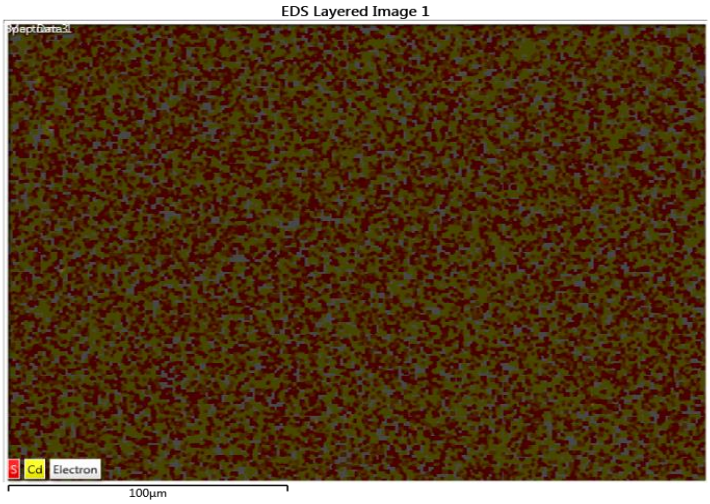

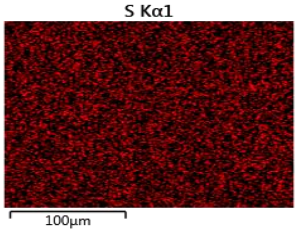

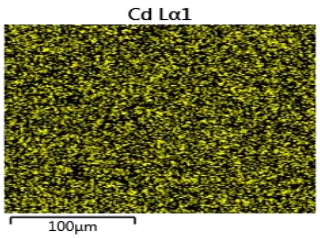

Low (inset) and high magnification SEM images: **7Fa** and **8F**

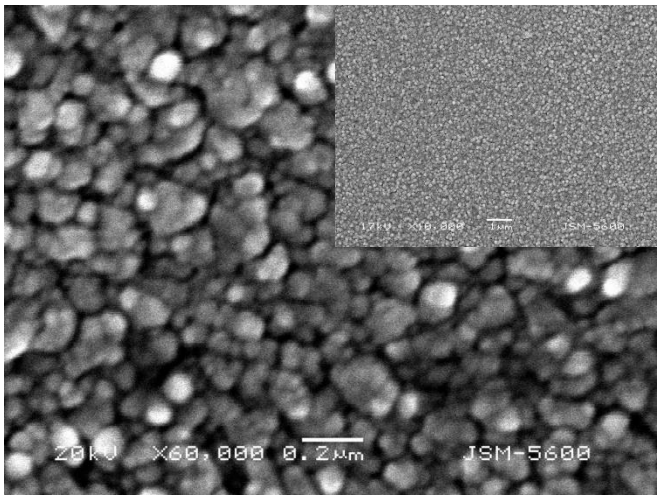

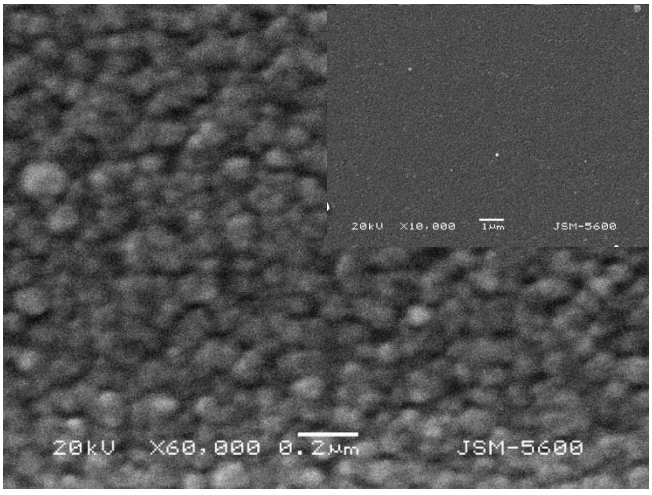

8F Elemental Mapping (SEM), sulfur, cadmium and subtrate: silicium and oxigen.

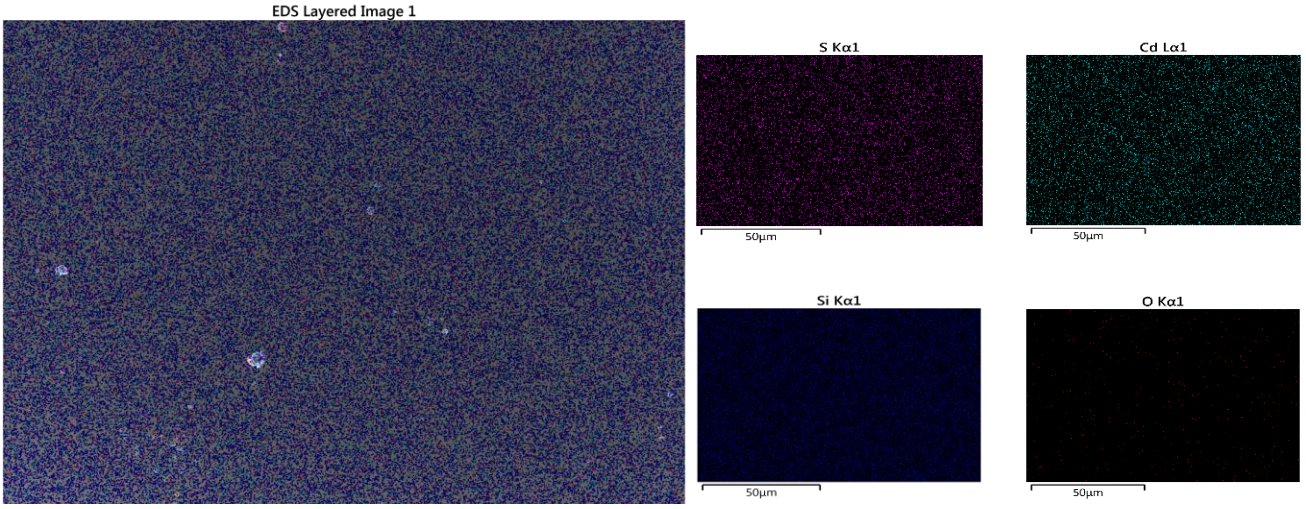

Low (inset) and high magnification SEM images: **8Fa**

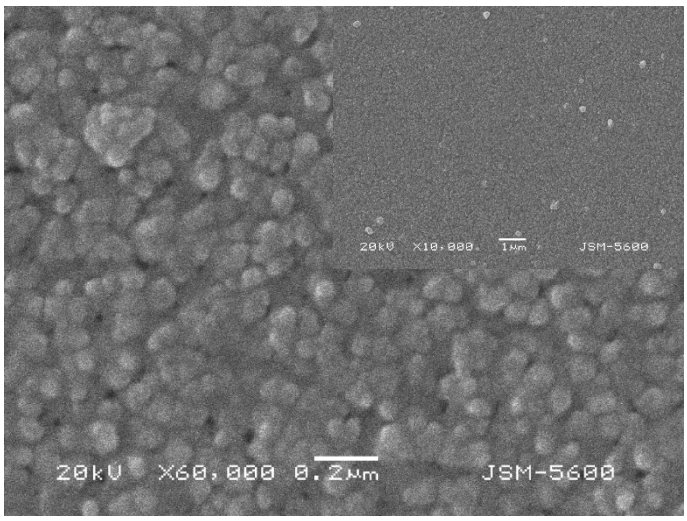

AFM micrograph (1 x 1 µm, inset10 x 10 µm): **8Fa**

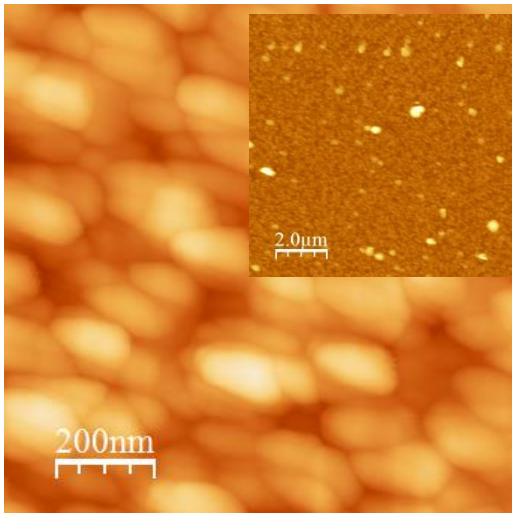

Low (inset) and high magnification SEM images: **9F**

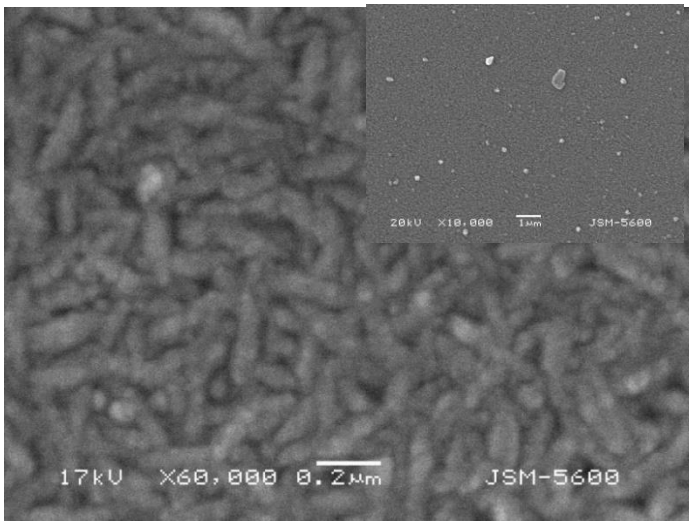

AFM micrograph (10 x 10 µm): **9F**

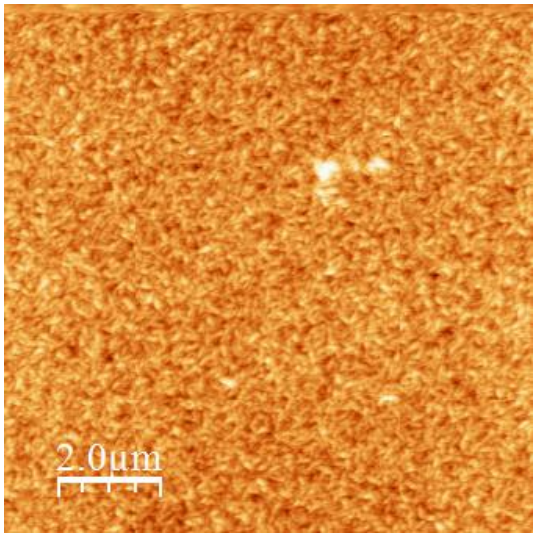

Low (inset) and high magnification SEM images: **9Fa**

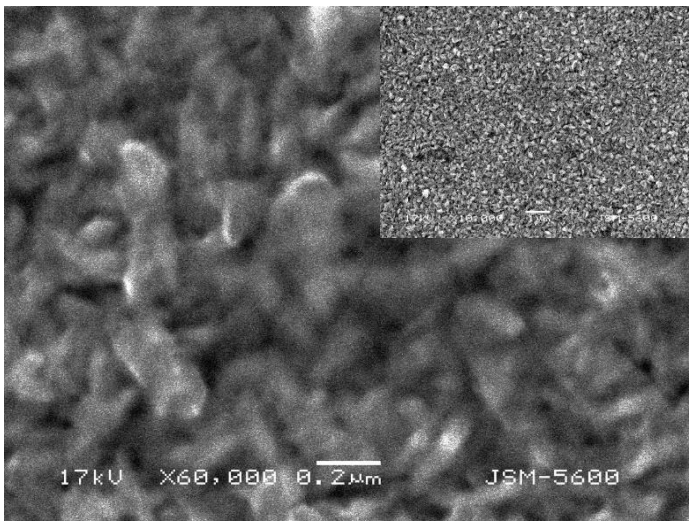

AFM micrograph (2 × 2 µm, inset 5 × 5 µm): **9Fa**

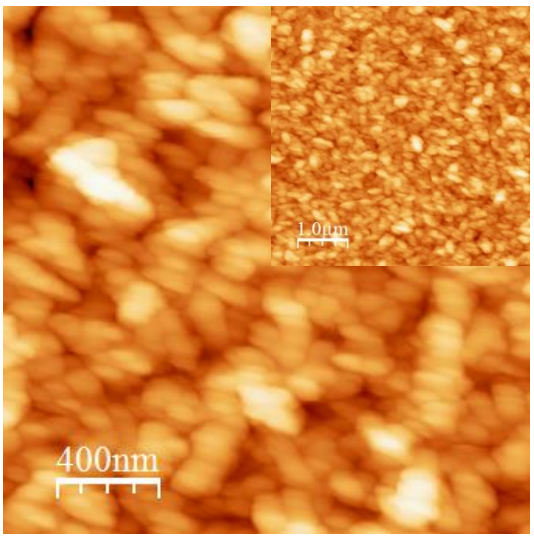

4. X-ray diffraction structural analysis. The average crystallite size was calculated from Debye–Scherrer equation (1) 2 for all unannealed thin films produced at 450°C (**4F**-**9F**) and the corresponding annealed films at 600°C (**4F-a**-**9F-a**).

$$D = \frac{0.94\lambda}{\beta \cos\theta} \qquad (1)$$

where λ is the wavelength of the X-ray used; β is the width of the peak at half the maximum intensity in radians and θ is the Bragg diffraction angle. The strain (ε) and grain size of the samples were calculated by the Williamson–Hall (W–H) relation,[1] according to the following equation (2)

$$\beta cos\theta = \frac{K\lambda}{D} + 4\varepsilon\, sin\theta \qquad (2)$$

The strain is estimated from the slope of the plots of β cosθ/λ *versus* sinθ/λ, while the crystallite size (D) from the intercept on the Y-axis

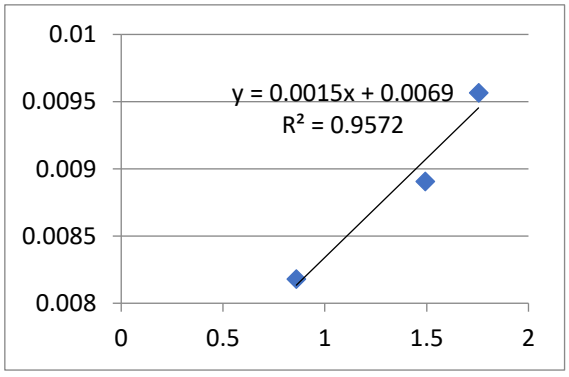

X	Y
4sinθ	βcosθ
0.85996405	0.00818168
1.49259886	0.00890596
1.75473943	0.00956739

Figure S3. Williamson–Hall plot for **9F**

5. The optical band gap (Eg) were estimated using Tauc's relationship:[2]

$$\alpha h\nu = B(h\nu - E_g)^{1/m} \qquad (4)$$

where α is the absorption coefficient, hν is the incident photon energy, B is the energy-dependent constant, E_g is the optical band gap of the material, and m is the transition coefficient which can be 1/2, 3/2, 2, and 3, in this case m = 1/2 for direct allowed transitions and α was evaluated using the following relation

$$\alpha = -\frac{1}{t}\ln T \qquad (5)$$

$$E_{phonon} = \frac{hC}{\lambda} \qquad (6)$$

where t is the film thickness, T the transmittance. The optical energy gap, E_g of the investigated MS thin films, were obtained from plot $(\alpha h\nu)^2$ versus the photon energy (hν) by extrapolating linear part to intersect (hν) axis at $(\alpha h\nu)^2 = 0$ (Figure S4 for annealed films).

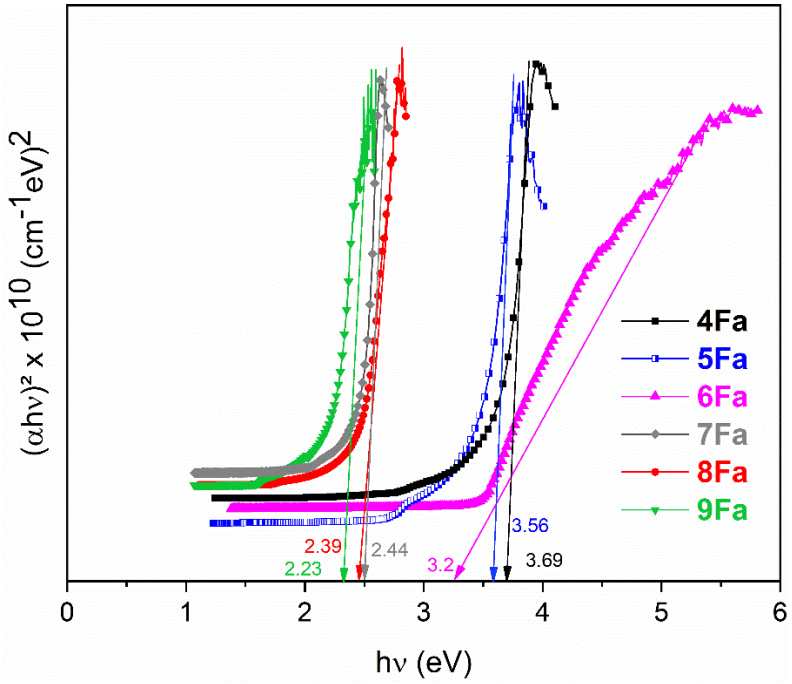

Figure S4. $(\alpha h\nu)^2$ vs hν plot showing the estimated optical band gap of annealed films (600 °C) **4Fa**–**9Fa**.

6. **Table 2.** Band gap (E_g) of our films and reported MS thin films obtained from different SSPs and techniques.

M	Precursor	Preparation method (solvent)	T_{prep} (°C)	Eg (eV)	Ref
Zn	**4**	AACVD (Toluene)	450	3.9	*
Zn	**4**		annealed (600)	3.69	*
Zn	**5**		450	3.64	*
Zn	**5**		annealed (600)	3.56	*
Zn	**6**		450	3.43	*

Zn	**6**		annealed (600)	3.2	*
Zn	$Zn(N(SCNMe_2)_2)_2$	AACVD (THF)	300-450	3.23, 3.36	[3]
Zn	$Zn(N(SCNEt_2)_2)_2$		300-450	2.62 -3.21	[3]
Zn	$Zn(NSO(CN^iPr_2)_2)_2$		300-450	3.23 -3.31	[3]
Zn	$Zn(^iPr_2P(S)NHP(S)^iPr_2P)_2$	LP-MOCVD	450	3.64	[4]
Zn	$[Zn(SOCPh)_2lutidine_2{\cdot}H_2O]$	One-step thermal decomposition	600	3.58	[5]
Zn	$Zn(C_{10}H_{11}N_3S)_2$	AACVD (methanol)	400-500	3.70	[6]
Zn	$Zn(C_8H_8ClN_3S)_2$		400-500	3.91	[6]
Zn	$[Zn\{^iPrNC(S)NMe_2\}_2]_2$	AACVD (THF)	200-350	3.71-3.79	[7]
Cd	**7**	AACVD (Toluene)	450	2.5	*
Cd	**7**		annealed (600)	2.44	*
Cd	**8**		450	2.44	*
Cd	**8**		annealed (600)	2.39	*
Cd	**9**		450	2.28	*
Cd	**9**		annealed (600)	2.23	*
Cd	$Cd(N(SCNMe_2)_2)_2$	AACVD (THF)	350-500	2.41-2.43	[3]
Cd	$Cd(N(SCNEt_2)_2)_2$		350-500	2.32-2.41	[3]
Cd	$Cd(NSO(CN^iPr_2)_2)_2$		350-500	2.34-2.41	[3]
Cd	$Cd(^iPr_2P(S)NHP(S)^iPr_2P)_2$	LP-MOCVD	450	2.30	[4]
Cd	$Cd[S_2CNCy_2]_2{\cdot}py$	AACVD (pyridine)	350-450	2.4	[8]
Cd	$Cd[S_2CNC_5H_{10}]_2{\cdot}py$	AACVD (chloroform)	350-450	2.4	[9]
Cd	$Cd[S_2CN(C_6H_{13})_2]_2{\cdot}$	AACVD (THF)	400/450	2.43/2.41	[10]
Cd	$Cd[S_2CNEt_2]_2{\cdot}$		400/450	2.41/2.42	[10]
Cd	$Cd[S_2C(NC_5H_{10})]_2$		400/450	2.37/2.40	[10]
Cd	$Cd[EtOCS_2]_2$		400/450	2.44/2.49	[10]
Cd	$Cd[EtOCS_2]_2$ R-py_2	AACVD (THF)	220 and 350	2.25-2.40	[11]
Cd	$Cd(EtOCS_2)_2py_2$	Thermolysis/annealed	150/350	2.4	[12]

*This work

7. **Figure S5.** Raman spectra of annealed CdS films (**7Fa** - **9Fa**) under 488 nm excitation.

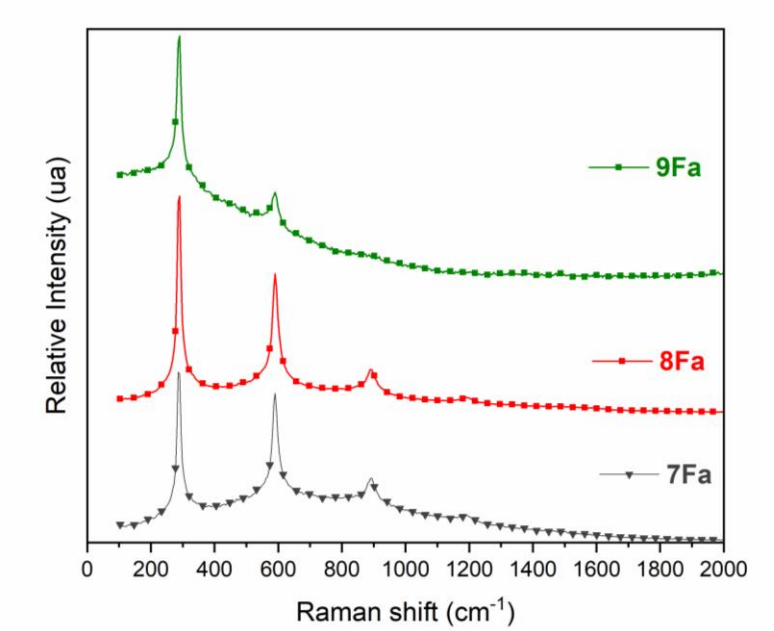

8. **Figure S6.** PL spectra (λ_{exc} = 488 nm) of as-deposited ZnS films: **5F** and **6F** (450℃).

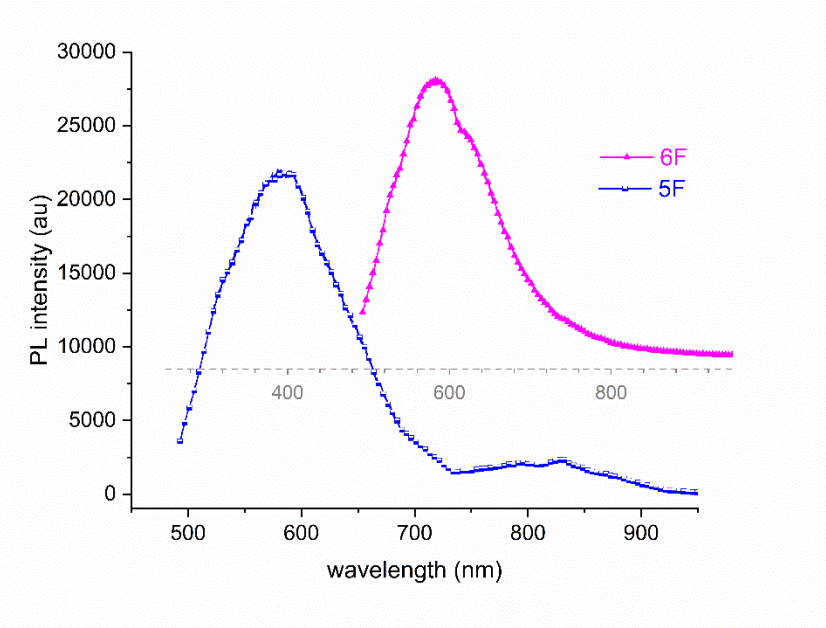

Notes and references

1 F. A. La Porta, J. Andrés, M. S. Li, J. R. Sambrano, J. A. Varela and E. Longo, *Phys. Chem. Chem. Phys.*, 2014, **16**, 20127–20137.

2 A. S. Hassanien, K. A. Aly and A. A. Akl, *J. Alloys Compd.*, 2016, **685**, 733–742.

3 K. Ramasamy, M. A. Malik, M. Helliwell, J. Raftery, P. O'Brien, P. O. Brien, A. Zinc and P. O'Brien, *Chem. Mater.*, 2011, **23**, 1471–1481.

4 M. Afzaal, D. Crouch, M. A. Malik, M. Motevalli, P. O'Brien, J.-H. H. Park, J. D. Woollins, P. O'Brien, J.-H. Park and J. D. Woollins, *Eur. J. Inorg. Chem.*, 2004, 171–177.

5 S. K. Maji, N. Mukherjee, A. Mondal, B. Adhikary, B. Karmakar and S. Dutta, *Inorganica Chim. Acta*, 2011, **371**, 20–26.

6 A. M. Palve, *Front. Mater.*, 2019, **6**, 1–7.

7 H. S. I. Sullivan, J. D. Parish, P. Thongchai, G. Kociok-Köhn, M. S. Hill and A. L. Johnson, *Inorg. Chem.*, 2019, **58**, 2784–2797.

8 M. A. Ehsan, H. N. Ming, M. Misran, Z. Arifin, E. R. T. Tiekink, A. P. Safwan, M. Ebadi, W. J. Basirun and M. Mazhar, *Chem. Vap. Depos.*, 2012, **18**, 191–200.

9 S. Mlowe, D. J. Lewis, M. Azad Malik, J. Raftery, E. B. Mubofu, P. O'Brien and N. Revaprasadu, *New J. Chem.*, 2014, **38**, 6073–6080.

10 K. I. Y. Ketchemen, S. Mlowe, L. D. Nyamen, P. T. Ndifon, N. Revaprasadu and P. O'Brien, *J. Mater. Sci. Mater. Electron.*, 2018, **29**, 14462–14470.

11 M. A. Buckingham, A. L. Catherall, M. S. Hill, A. L. Johnson and J. D. Parish, *Cryst. Growth Des.*, 2017, **17**, 907–912.

12 A. S. R. Chesman, N. W. Duffy, A. Martucci, L. De Oliveira Tozi, T. B. Singh and J. J. Jasieniak, *J. Mater. Chem. C*, 2014, **2**, 3247–3253.